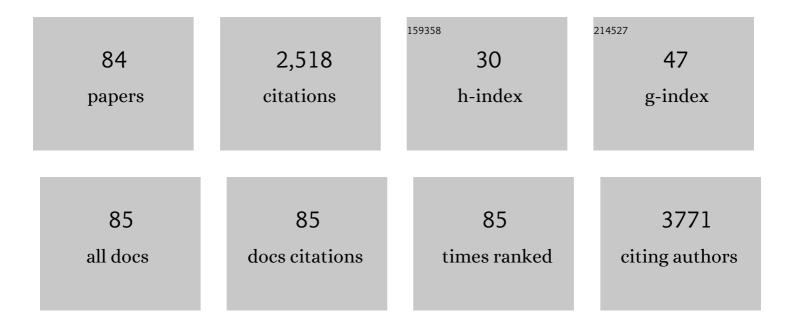
List of Publications by Year in descending order

Source: https://exaly.com/author-pdf/7502809/publications.pdf Version: 2024-02-01



PAOLA RIVOLO

#	Article	IF	CITATIONS
1	Effective Inclusion of Sizable Amounts of Mo within TiO <sub>2</sub> Nanoparticles Can Be Obtained by Reverse Micelle Sol–Gel Synthesis. ACS Omega, 2021, 6, 5379-5388.	1.6	16
2	Reverse Micelle Strategy for the Synthesis of MnO <sub><i>x</i></sub> –TiO <sub>2</sub> Active Catalysts for NH <sub>3</sub> -Selective Catalytic Reduction of NO <sub><i>x</i></sub> at Both Low Temperature and Low Mn Content. ACS Omega, 2021, 6, 24562-24574.	1.6	12
3	Real-Time Monitoring of the In Situ Microfluidic Synthesis of Ag Nanoparticles on Solid Substrate for Reliable SERS Detection. Biosensors, 2021, 11, 520.	2.3	2
4	Beta1-integrin and TRPV4 are involved in osteoblast adhesion to different titanium surface topographies. Applied Surface Science, 2020, 507, 145112.	3.1	8
5	Binder Free and Flexible Asymmetric Supercapacitor Exploiting Mn3O4 and MoS2 Nanoflakes on Carbon Fibers. Nanomaterials, 2020, 10, 1084.	1.9	30
6	Graphenic Aerogels Decorated with Ag Nanoparticles as 3D SERS Substrates for Biosensing. Particle and Particle Systems Characterization, 2020, 37, 2000095.	1.2	9
7	A Facile and Green Synthesis of a MoO2-Reduced Graphene Oxide Aerogel for Energy Storage Devices. Materials, 2020, 13, 594.	1.3	20
8	New branched flower-like Ag nanostructures for SERS analysis. Colloids and Surfaces A: Physicochemical and Engineering Aspects, 2019, 578, 123600.	2.3	21
9	Lift-Off Assisted Patterning of Few Layers Graphene. Micromachines, 2019, 10, 426.	1.4	7
10	Cysteine-mediated synthesis of silver nanonets and their use for Surface Enhanced Raman Scattering (SERS). Materials Letters, 2019, 247, 208-210.	1.3	4
11	Application of Reverse Micelle Sol–Gel Synthesis for Bulk Doping and Heteroatoms Surface Enrichment in Mo-Doped TiO2 Nanoparticles. Materials, 2019, 12, 937.	1.3	21
12	Tips and Tricks for the Surface Engineering of Wellâ€Ordered Morphologically Driven Silverâ€Based Nanomaterials. ChemistryOpen, 2019, 8, 508-519.	0.9	6
13	Modeling of electrochemical capacitors under dynamical cycling. Electrochimica Acta, 2019, 296, 709-718.	2.6	7
14	Fiber-shaped asymmetric supercapacitor exploiting rGO/Fe2O3 aerogel and electrodeposited MnOx nanosheets on carbon fibers. Carbon, 2019, 144, 91-100.	5.4	61
15	Hydrogenated amorphous silicon coatings may modulate gingival cell response. Applied Surface Science, 2018, 436, 603-612.	3.1	15
16	Bloch surface wave label-free and fluorescence platform for the detection of VEGF biomarker in biological matrices. Sensors and Actuators B: Chemical, 2018, 255, 2143-2150.	4.0	25
17	Early Response of Fibroblasts and Epithelial Cells to Pink-Shaded Anodized Dental Implant Abutments: An In Vitro Study. International Journal of Oral and Maxillofacial Implants, 2018, 33, 571-579.	0.6	27
18	Bloch surface wave enhanced biosensor for the direct detection of Angiopoietin-2 tumor biomarker in human plasma. Biomedical Optics Express, 2018, 9, 529.	1.5	19

#	Article	IF	CITATIONS
19	Graphene/Ruthenium Active Species Aerogel as Electrode for Supercapacitor Applications. Materials, 2018, 11, 57.	1.3	21
20	Beneficial effect of Fe addition on the catalytic activity of electrodeposited MnOx films in the water oxidation reaction. Electrochimica Acta, 2018, 284, 294-302.	2.6	13
21	High-Performing and Stable Wearable Supercapacitor Exploiting rGO Aerogel Decorated with Copper and Molybdenum Sulfides on Carbon Fibers. ACS Applied Energy Materials, 2018, 1, 4440-4447.	2.5	88
22	In vitro characterization of two different atmospheric plasma jet chemical functionalizations of titanium surfaces. Applied Surface Science, 2017, 409, 314-324.	3.1	24
23	SERS-active metal-dielectric nanostructures integrated in microfluidic devices for label-free quantitative detection of miRNA. Faraday Discussions, 2017, 205, 271-289.	1.6	39
24	SERS-active Metal-dielectric Nanostructures Integrated in Microfluidic Devices for Ultra-sensitive Label-free miRNA Detection. Procedia Technology, 2017, 27, 37-38.	1.1	0
25	Graphene-Metal Nanostructures as Surface Enhanced Raman Scattering Substrates for Biosensing. Procedia Technology, 2017, 27, 236-237.	1.1	0
26	Multiple resistive switching in core–shell ZnO nanowires exhibiting tunable surface states. Journal of Materials Chemistry C, 2017, 5, 10517-10523.	2.7	40
27	Role of surface finishing on the in vitro biological properties of a silicon nitride–titanium nitride (Si3N4–TiN) composite. Journal of Materials Science, 2017, 52, 467-477.	1.7	20
28	Surface Treatments and Functional Coatings for Biocompatibility Improvement and Bacterial Adhesion Reduction in Dental Implantology. Coatings, 2016, 6, 7.	1.2	113
29	Ultra-Thin Plasma-Polymerized Functional Coatings for Biosensing: Polyacrylic Acid, Polystyrene and Their Co-Polymer. , 2016, , .		2
30	Memristive behaviour in poly-acrylic acid coated TiO <sub>2</sub> nanotube arrays. Nanotechnology, 2016, 27, 485208.	1.3	24
31	Optimization and characterization of a homogeneous carboxylic surface functionalization for silicon-based biosensing. Colloids and Surfaces B: Biointerfaces, 2016, 143, 252-259.	2.5	20
32	A novel graphene based nanocomposite for application in 3D flexible micro-supercapacitors. Materials Research Express, 2016, 3, 065001.	0.8	11
33	Immobilization of Oligonucleotides on Metal-Dielectric Nanostructures for miRNA Detection. Analytical Chemistry, 2016, 88, 9554-9563.	3.2	41
34	Hydrophobic Scratch Resistant UV-Cured Epoxy Coating. Macromolecular Materials and Engineering, 2016, 301, 93-98.	1.7	4
35	SERS-Active Ag Nanoparticles on Porous Silicon and PDMS Substrates: A Comparative Study of Uniformity and Raman Efficiency. Journal of Physical Chemistry C, 2016, 120, 16946-16953.	1.5	57
36	Optical and structural properties of amorphous silicon-nitrides and silicon-oxycarbides: Application of multilayer structures for the coupling of Bloch Surface Waves. Journal of Non-Crystalline Solids, 2016, 453, 113-117.	1.5	11

#	Article	IF	CITATIONS
37	Mixed 1T–2H Phase MoS <sub>2</sub> /Reduced Graphene Oxide as Active Electrode for Enhanced Supercapacitive Performance. ACS Applied Materials & Interfaces, 2016, 8, 32842-32852.	4.0	132
38	Optical Sensing with All-Dielectric Photonic Crystals. , 2016, , .		0
39	Study of the adhesive properties versus stability/aging of hernia repair meshes after deposition of RF activated plasma polymerized acrylic acid coating. Materials Science and Engineering C, 2016, 65, 287-294.	3.8	10
40	Surface-enhanced Raman spectroscopy on porous silicon membranes decorated with Ag nanoparticles integrated in elastomeric microfluidic chips. RSC Advances, 2016, 6, 21865-21870.	1.7	32
41	Easy Tuning of Surface and Optical Properties of PDMS Decorated by Ag Nanoparticles. Journal of Physical Chemistry B, 2015, 119, 8194-8200.	1.2	32
42	Ultrasensitive Ag-coated TiO <sub>2</sub> nanotube arrays for flexible SERS-based optofluidic devices. Journal of Materials Chemistry C, 2015, 3, 6868-6875.	2.7	54
43	Surface functionalisation of polypropylene hernia-repair meshes by RF-activated plasma polymerisation of acrylic acid and silver nanoparticles. Applied Surface Science, 2015, 328, 287-295.	3.1	32
44	Angularly resolved ellipsometric optical biosensing by means of Bloch surface waves. Analytical and Bioanalytical Chemistry, 2015, 407, 3965-3974.	1.9	25
45	Enhanced fluorescence detection of miRNA-16 on a photonic crystal. Analyst, The, 2015, 140, 5459-5463.	1.7	31
46	New Sensing Strategies Based on Surface Modes in Photonic Crystals. , 2015, , 321-337.		1
47	SERS active silver nanoparticles synthesized by inkjet printing on mesoporous silicon. Nanoscale Research Letters, 2014, 9, 527.	3.1	40
48	Bloch Surface Waves on Dielectric Photonic Crystals for Biological Sensing. Lecture Notes in Electrical Engineering, 2014, , 107-111.	0.3	0
49	Inkjet-printed PEDOT:PSS electrodes on plasma-modified PDMS nanocomposites: quantifying plasma treatment hardness. RSC Advances, 2014, 4, 51477-51485.	1.7	61
50	Fluorescence imaging assisted by surface modes on dielectric multilayers. European Physical Journal D, 2014, 68, 1.	0.6	6
51	Protein immobilization on nanoporous silicon functionalized by RF activated plasma polymerization of Acrylic Acid. Journal of Colloid and Interface Science, 2014, 416, 73-80.	5.0	25
52	Silver Nanoparticles on Porous Silicon: Approaching Single Molecule Detection in Resonant SERS Regime. Journal of Physical Chemistry C, 2013, 117, 20139-20145.	1.5	63
53	A Fluorescent One-Dimensional Photonic Crystal for Label-Free Biosensing Based on Bloch Surface Waves. Sensors, 2013, 13, 2011-2022.	2.1	56
54	A polymer-based functional pattern on one-dimensional photonic crystals for photon sorting of fluorescence radiation. Optics Express, 2012, 20, 6703.	1.7	29

#	Article	IF	CITATIONS
55	Controlled fluorescence emission via surface modes on dielectric and metallo-dielectric multistack. , 2012, , .		0
56	Switching of fluorescence mediated by a peroxynitrite–glutathione redox reaction in a porous silicon nanoreactor. Physical Chemistry Chemical Physics, 2012, 14, 5251.	1.3	7
57	Direct patterning of silver particles on porous silicon by inkjet printing of a silver salt via in-situ reduction. Nanoscale Research Letters, 2012, 7, 502.	3.1	48
58	Surface functionalization by poly-acrylic acid plasma-polymerized films for microarray DNA diagnostics. Surface and Coatings Technology, 2012, 207, 389-399.	2.2	31
59	SERS active Ag nanoparticles in mesoporous silicon: detection of organic molecules and peptide–antibody assays. Journal of Raman Spectroscopy, 2012, 43, 730-736.	1.2	70
60	Surface modification of cell culture carriers: Routes to anhydride functionalization of polystyrene. Colloids and Surfaces B: Biointerfaces, 2012, 90, 41-47.	2.5	15
61	Real time secondary antibody detection by means of silicon-based multilayers sustaining Bloch surface waves. Sensors and Actuators B: Chemical, 2012, 161, 1046-1052.	4.0	54
62	Inkjet printing and low power laser annealing of silver nanoparticle traces for the realization of low resistivity lines for flexible electronics. Microelectronic Engineering, 2011, 88, 2481-2483.	1.1	106
63	Bloch surface waves-controlled emission of organic dyes grafted on a one-dimensional photonic crystal. Applied Physics Letters, 2011, 99, .	1.5	75
64	SERSâ€active substrates based on silvered porous silicon. Physica Status Solidi C: Current Topics in Solid State Physics, 2009, 6, 1736-1739.	0.8	21
65	Doubly resonant porous silicon microcavities for enhanced detection of fluorescent organic molecules. Sensors and Actuators B: Chemical, 2009, 137, 467-470.	4.0	39
66	On diamond surface properties and interactions with neurons. European Physical Journal E, 2009, 30, 149-56.	0.7	31
67	A biofunctional polymeric coating for microcantilever molecular recognition. Analytica Chimica Acta, 2008, 630, 161-167.	2.6	39
68	Vapor-phase self-assembled monolayers of aminosilane on plasma-activated silicon substrates. Journal of Colloid and Interface Science, 2008, 321, 235-241.	5.0	126
69	SiNx/a-SiCx:H passivation layers for p- and n-type crystalline silicon wafers. Thin Solid Films, 2008, 516, 1569-1573.	0.8	3
70	Study of Porous Silicon Nanostructures as Hydrogen Reservoirs ChemInform, 2006, 37, no.	0.1	0
71	A Nanostructured Porous Silicon Near Insulator Becomes Either a p- or an n-Type Semiconductor upon Gas Adsorption. Advanced Materials, 2005, 17, 528-531.	11.1	51
72	Carriers reactivation in p+-type porous silicon accompanies hydrogen desorption. Physica Status Solidi C: Current Topics in Solid State Physics, 2005, 2, 3193-3197.	0.8	1

#	Article	IF	CITATIONS
73	Boron passivation and its reactivation in mesoporous silicon: a "chemical―model. Physica Status Solidi (A) Applications and Materials Science, 2005, 202, 1567-1570.	0.8	5
74	Study of Porous Silicon Nanostructures as Hydrogen Reservoirs. Journal of Physical Chemistry B, 2005, 109, 19711-19718.	1.2	80
75	A new route to the surface functionalisation of porous silicon. Sensors and Actuators B: Chemical, 2004, 100, 29-32.	4.0	11
76	Free carriers reactivation on p+-mesoporous silicon through ammonia adsorption: a FTIR study. Sensors and Actuators B: Chemical, 2004, 100, 205-208.	4.0	17
77	Oxidised porous silicon impregnated with Congo Red for chemical sensoring applications. Sensors and Actuators B: Chemical, 2004, 100, 99-102.	4.0	31
78	Chemisorption of NO2at Boron Sites at the Surface of Nanostructured Mesoporous Silicon. Journal of Physical Chemistry B, 2004, 108, 18306-18310.	1.2	12
79	Porous silicon in NO2: A chemisorption mechanism for enhanced electrical conductivity. Physica Status Solidi A, 2003, 197, 103-106.	1.7	15
80	Joint FTIR and TPD study of hydrogen desorption from p-type porous silicon. Physica Status Solidi A, 2003, 197, 217-221.	1.7	25
81	Free carriers reactivation in mesoporous p-type silicon by ammonia condensation: an FTIR study. Physica Status Solidi A, 2003, 197, 458-461.	1.7	10
82	IR detection of NO2 using p+ porous silicon as a high sensitivity sensor. Chemical Communications, 2001, , 2196-2197.	2.2	25
83	Local environment of Boron impurities in porous silicon and their interaction withNO2molecules. Physical Review B, 2001, 64, .	1.1	54
84	Nature and reactivity of Co species in a cobalt-containing beta zeolite: an FTIR study. Catalysis Today, 2001, 70, 107-119.	2.2	47